Grenze International Journal of Engineering and Technology, Jul 2019

Real-Time Particle Swarm Optimization based Parallel Hybrid Active Power Filter under Variable Load Conditions

Satya Prakash Dubey [1] and Kapil Kumar Nagwanshi[2]
[1] Rungta College of Engineering & Technology, Bhilai, CG 490024 INDIA
Email: spd1020@yahoo.com
[2] MPSTME, SVKM's NMIMS University, Shirpur Campus, India ame of Institution/Department, City, Country
Email: kapilkn@ieee.org

***Abstract*—In electrical distribution system, nonlinear loads draw reactive power and / or undesired harmonic currents from ac source along with the fundamental current. Various power quality compensators are being considered as potential candidate for solving such power quality problems not only in ideal supply but also in distorted supply conditions. This paper presents a new method for harmonic and reactive power compensation using a Particle Swarm Optimization (PSO) algorithm for Parallel Hybrid Active Power Filter (HAPF) for power quality improvement under dynamic loading and non-ideal mains conditions. The PSO comprises two similar swarm group (swarm size-25), and it has been designed to extract fundamental frequency components from non-sinusoidal and unbalanced currents instead of conventional low pass filter. The reactive power compensation is done without sensing load currents, which gives simplicity in control with less number of current sensors. The performance of the parallel HAPF with the proposed particle swarm optimization compensation algorithm is found to be considerably effective and adequate to compensate harmonics and reactive power. The experimental results show excellent behavior of PSO based controller and performances of parallel HAPF under various load conditions.**

***Index Terms*— Artificial Neural Network; Fast Fourier Transform; Particle Swarm Optimization; Power filter; Total Harmonic Distortion.**

I. INTRODUCTION

In electrical supply system, customer must receive continuous fundamental sinusoidal voltage of constant magnitude. Due to numerous nonlinear power electronics loads, harmonics are injected in system. The injected harmonics in power system leads to malfunctioning and heating of devices. Therefore, it is required to reduce the total harmonic distortion below 5% as specified in IEEE 519-1992 harmonic standard [1]. The passive and active filters are being used to filter out the harmonics in power distribution system. According to Grady et al (1990), and Peng et al (1990), the implementation of passive filter is easier but dependency on source and load characteristics and resonance problem makes them less viable [2][3]. The complexity in realization of active power filter is high, but harmonics can be removed effectively. Hybrid active power filter consists of passive tuned filter and active filter. The compensation characteristics of passive tuned filter is improved by active power

Grenze ID: 01.GIJET.5.2.2

filter at relatively at lower cost than alone shunt active power filter due to device ratings. The accuracy of reference signal and computation speed strongly affects the filtering characteristics of active power filter. Based on Fast Fourier Transform (FFT), Kalman filter, and Artificial Neural Network (ANN) various reference generation schemes have been designed and developed to control the HAPF. Practically signal is contaminated by noise and DC component of decaying signal, reference signal generation using FFT leads to inaccurate results. The reference signal calculation based on Kalman filter is not suitable for on line applications because of high computational demand due to transcendental function evaluations [4]. The ANNs based harmonic reference signal estimation requires excessive data for training, which may lead to inaccurate results due to random noise. Marks and Green (2002), describes Neuro-Fuzzy based schemes and found complex plus difficult in realization in distorted supply system [5]. This paper presents a three-phase three-wire swarm intelligence controlled parallel hybrid active filters [6]. The proposed swarm intelligence based controller for reference signal generation is self-adapting in nature, fast, and simple in architecture [7,8]. Gupta et al (2011), developed a neural network-based shunt active filter with direct current control for power quality conditioning, and also a swarm particle-based controller has designed, modeled and evaluated under all possible nonlinear and unbalanced source and load conditions [9].

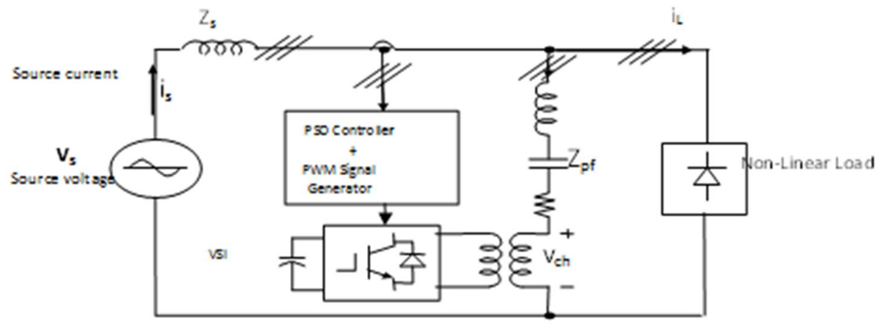

Fig. 1. Single phase equivalent of three-phase proposed PSO Controlled Hybrid Active Power filter

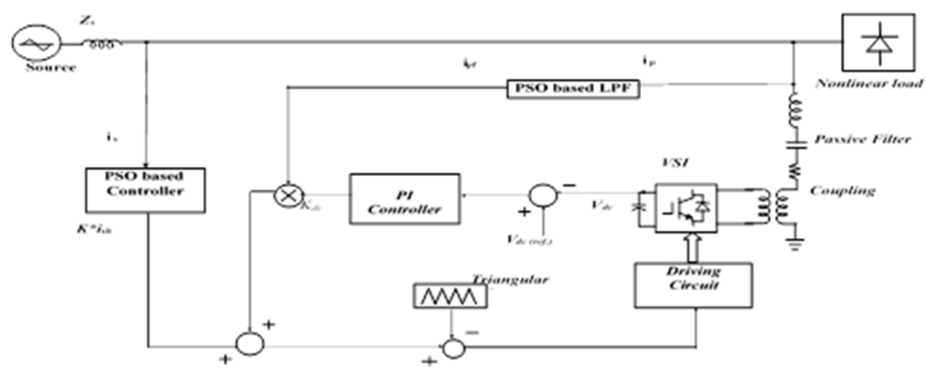

Fig. 2. Control block diagram of the proposed hybrid active power filter

II. Formulation of Problem

Fig.1 presents the general topology of the proposed system. It mainly consists of a 3-phase insulated-gate bipolar transistor (IGBT) based voltage source inverter (VSI); PSO based harmonic current calculator and passive filters tuned at 5th, 7th and 11th harmonics. The VSI generates control voltage $V_{c\square} = (K \times i_{s\square})$ and injects this through coupling transformer in series with passive tuned filters. This improves the compensation characteristics of passive filters and overcome most of the drawbacks of using passive filters alone. The PSO controller extracts the fundamental components from source currentsi_s. The extracted fundamental currents subtracted from source currents i_s to compute the reference signal i.e. harmonic componentsi_{sh}. Singh (2001), has found the relationship among source side harmonic currents, load harmonic current i_{Lh} and the source harmonic voltage $V_{s\square}$, which has been described as eq. (1):

$$i_{s\square} = \frac{Z_{pf}}{Z_{pf}+Z_s+K} \times i_{L\square} + \frac{1}{Z_{pf}+Z_s+K} \times V_{s\square} \quad (1)$$

where Z_{pf} and Z_s are the impedances of passive filter and source respectively as shown in Fig. 1, where K is the gain of Hybrid Active Power Filter (HAPF). If$K >> |Z_{pf} + Z_s|$, then harmonic components of source current $I_{sh} \cong 0$ and $V_{s\square}$ would be applied to the active filter[10]. The filtering performance up to a great where Z_{pf} and Z_s are the impedances of passive filter and source respectively as shown in Fig. 1, where K is the gain of Hybrid Active Power Filter (HAPF). If$K >> |Z_{pf} + Z_s|$, then harmonic components of source current $I_{sh} \cong 0$ and $V_{s\square}$ would be applied to the active filter[10]. The filtering performance up to a great extent is not influenced by the source or passive filter impedance.

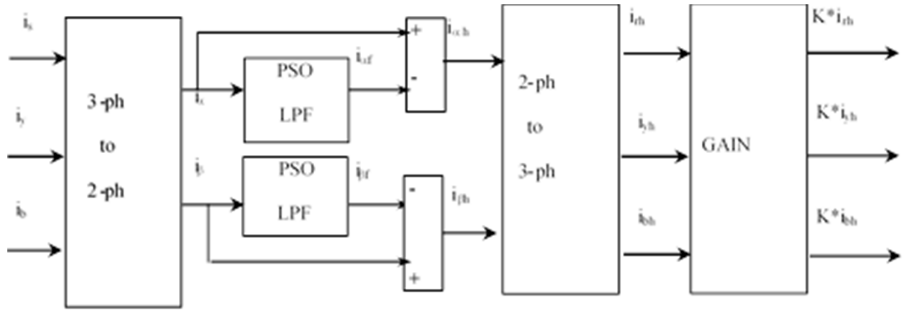

Figure 3. Block diagram of PSO based extraction network

III. SOLUTION METHODOLOGY

Fig. 2, shows the control circuit diagram of the hybrid active filter. Based on method established by Lin (2002), and Singh et al (2001), there are two control blocks, one is the harmonic suppression block to eliminate the nonlinear harmonic current, and the other is the dc voltage control block to maintain a constant dc bus voltage [11,12]. In the harmonic suppression loop, a PSO based filter is used to obtain the source fundamental current. In the dc voltage control loop, a PI voltage controller is employed [13,14]. The block diagram of proposed PSO based controller is shown in Fig. 3. The three phase source currentsi_r, i_v, and i_b are first transformed into two phase currents i_α and i_β using eq. (2):

$$\begin{bmatrix} i_\alpha \\ i_\beta \end{bmatrix} = \sqrt{\frac{2}{3}} \begin{bmatrix} 1 & -\frac{1}{2} & -\frac{1}{2} \\ 0 & \frac{\sqrt{3}}{2} & -\frac{\sqrt{3}}{2} \end{bmatrix} \begin{bmatrix} i_r \\ i_y \\ i_b \end{bmatrix} \quad (2)$$

$$\begin{bmatrix} i_{r\square} \\ i_{y\square} \\ i_{b\square} \end{bmatrix} = \sqrt{\frac{2}{3}} \begin{bmatrix} 1 & 0 \\ -\frac{1}{2} & \frac{\sqrt{3}}{2} \\ -\frac{1}{2} & -\frac{\sqrt{3}}{2} \end{bmatrix} \begin{bmatrix} i_{\alpha\square} \\ i_{\beta\square} \end{bmatrix} \quad (3)$$

The PSO based low pass filter extracts fundamental components of two-phase current $i_{\alpha f}$and$i_{\beta f}$. Subtracting the extracted fundamental currents $i_{\alpha f}$and $i_{\beta f}$ from the two phase source currents $i_\alpha$and i_β respectively, two phase harmonic currents $i_{\alpha h}$ and $i_{\beta fh}$ are obtained. Finally, these two-phase harmonic components are transformed into three phase using eq. (3). The output voltage of converter for harmonic current suppression is obtained from the multiplication of the calculated source harmonic current and the equivalent harmonic resistorK_h.The FIR filter structure is advantageous in achieving exactly linear-phase frequency responses. Due to known phase response of liner phase filter, the filter coefficients have to be optimized only with magnitude response. Eq. (4) represents characteristics equation of digital FIR filter is:

$$H(z) = \sum_{n=0}^{N} \square(n) z^{-n}, n = 0,1,\ldots,N \quad (4)$$

where N represents order of filter with (N+1) number of coefficients $h(n)$ of filter's impulse response, the design process assigns the values of $h(n)$ and represented by polynomial equation of order N. The dimension of optimization task becomes halves due to symmetry in $h(n)$ coefficients. During optimization, actually optimized coefficients are only$\left(\frac{N}{2} + 1\right)$. The required (N+1) coefficients can be obtained by concatenated the optimized coefficients. The magnitude of one in the pass band and of zero in the stop band defines the ideal filter. The frequency response error between ideal and designed filter gives the error function to update the coefficients values during optimization. In optimization algorithm, during every iteration, fitness error values of particle vectors are calculated to update the particle vectors with updated (new) coefficients$h(n)$. The final values of coefficients (n), obtained after fixed number of iteration or achieving fitness error below a specified value provides optimal filter. The eq. (5) shows the frequency response of the FIR digital filter:

$$H(e^{jw_k}) = \sum_{n=0}^{N} \quad (n)e^{-jw_k n}, n = 0,1,\ldots,N \tag{5}$$

where$w_k = \frac{2\pi k}{n}$; and $H(e^{jw_k})$ represents the Fourier transform complex vector. The frequency is sampled with N points between [0, π]. Eq. (6) gives the approximate error function that is used to update the optimal filter coefficients (n) in proposed model of PSO:

$$E(w) = G(w)[H_d(e^{jw}) - H_i(e^{jw})] \tag{6}$$

where $H_d(e^{jw})$ represents frequency response of the designed optimal filter; frequency response of the ideal filter is given by$H_i(e^{jw})$; whereas, $G(w)$ is the weight function required to provide different weight values to calculate approximate errors in different frequency bands. Eq. (7) gives $H_i(e^{jw})$ for ideal low pass filter:

$$H_i(e^{jw}) = \begin{cases} 1 & for \quad 0 \le w \le w_c \\ 0 & \quad ot \;\; erwise \end{cases} \tag{7}$$

where w_c is the cut-off frequency. Unlike genetic algorithm (GA), PSO is less prone to get trapped in local optima, because the development of PSO is based on simulation of bird flocking in multidimensional space [15,16,17]. Based on personal experience of particle, each bird (particle) evaluates individual best value called (*pbest*) and the best value so far in the group (*gbest*) among (*pbests*). Each particle (bird) updates its own position on the basis of distance (error) between the current position and the *pbest,* and current position and the *gbest*. Based on the initial chromosome population concept of GA, swarm optimization technique also required initial population of birds (real-coded particle vectors). According to the order of designed filter, each particle vector contains the information of normalized filter coefficients. Eq. (8), gives the relation for velocity modification of particle vector:

$$V_i^{(k+1)} = V_i^k + C_1 \times rand_1 \times (pbest_i^k - X_i^k) + C_2 \times rand_2 \times (gbest_i^k - X_i^k) \tag{8}$$

where V_i^k is the velocity of i^{th} particle vector at K^{th} iteration; C_1 and C_2 are the positive weighing factors; $rand_1$ and $rand_2$ are the random values between 0 and 1; X_i^k is the current position of the i^{th} particle vector (n) at k^{th} iteration. In solution space the modified searching point may be given as (9):

$$X_i^{(k+1)} = X_i^k V_i^{(k+1)} \tag{9}$$

Table I shows the parameters of proposed PSO architecture and Table 2 gives the value of optimized coefficients of low pass filter of order 40. Fig. 4 (a) shows the error convergence with respect to number of iterations of the proposed PSO architecture, error function is reducing rapidly, which shows the better design process and Fig. 4 (b) represents the frequency versus magnitude response of proposed PSO based LPF.

TABLE I : PSO PARAMETERS

Parameters	Value
Population Size	25
Iteration Cycle	100
C_1	0.5
C_2	0.5
h_{min} (minimum value of coefficient value)	-1
h_{max} (maximum value of coefficient value)	+1
Filter Order (N)	40

PSO based Hybrid Active Power Filter prototype for experimental purpose has been set up and tested as shown in Fig.5(a). The ADMC401Digital Signal Processor (DSP) from Analog devices has been selected for the implementation of the proposed control scheme [18]. This is a 16-bit fixed point DSP, with a block frequency of 26 MHz. It has several peripherals on its core suitable for this application, such as 8-channel 12-bit analog to

Table II: Optimized Co-Efficient Of The Fir Filter Of Order 40

Impulse Response Coefficient h(n)	Value	Impulse Response Coefficient h(n)	Value
h(1)=h(41)	-3.86032876835977e-17	h(11)=h(31)	1.90848011715699e-17
h(2)=h(40)	-0.0158180339976153	h(12)=h(30)	0.0363593166326960
h(3)=h(39)	-2.94093228824865e-17	h(13)=h(29)	-9.67414831536822e-18
h(4)=h(38)	0.0197318043261204	h(14)=h(28)	-0.0445135080133765
h(5)=h(37)	4.63446115954017e-17	h(15)=h(27)	1.16734349396492e-17
h(6)=h(36)	-0.0202774577934189	h(16)=h(26)	0.0646454710844601
h(7)=h(35)	4.01849931061748e-17	h(17)=h(25)	-6.23683947586199e-18
h(8)=h(34)	0.0254849927238418	h(18)=h(24)	-0.105135907439110
h(9)=h(33)	-5.27958579801016e-17	h(19)=h(23)	4.16681712719559e-17
h(10)=h(32)	-0.0279859905890589	h(20)=h(22)	0.319285326657569
		h(21)	0.500000000000000

digital converter with simultaneous sampling capability (conversion time: 2µs for all 8-channels), three phase PWM generation unit, event timer unit for time /frequency measurement, RAM, PIO and two high-speed serial ports. The PSO algorithm has been implemented in real time on this DSP. The source current is measured using in-built ADC. For correct measurement of current under source frequency variation, 120 samples / fundamental period of AC mains are taken while sampling time is calculated and updated every half cycle. The α-and β axis fundamental currents, which are the outputs of particle swarm optimization algorithm, are converted into three phase fundamental currents. The reference signals are obtained by subtracting the fundamental currents from source currents. These reference signals fed to PWM signal generator for generating switching signals for the IGBTs of APF [19,20]. The switching frequency for APF is 20 KHz. The total time for the calculation of reference signals, measurement of three-phase source current, digital to analog conversion and PWM generation, when measured was found nearly 5µs. This execution time is almost negligible as compared to the period of AC mains. The design specifications and circuit parameters used in prototype model are given in Fig. 5(b). Fig. 6(a) and (b), show the load and source current waveforms for unbalance loading (R+L+ Motor). The snapshots of harmonic spectrum of load and source currents are depicted in Fig. 6(c) and (d). The THD after harmonic filtering, calculated using the data of Fig. 6(d), is found to be less than 4%. The comparison of Fig. 6(c) and 6(d) proves that the proposed HAPF can make source currents sinusoidal even in case of internal fault as the one considered in this investigation [21]. The small notching observed in Fig. 6(c) in the source current waveforms may be due to the presence of nonlinear load in the form of rectifier. Further, it is observed from this figure that the displacement power factor is very close to unity. The reason is that the fundamental frequency reactive power generated by the passive filters is nearly equal to the load reactive power. In Fig. 7 (a) and (b), the HAPF is in operation and compensating the harmonics generated by a balanced nonlinear load. The AC source feeding this load is balanced. Suddenly a three-phase unbalance load is connected to the AC mains. The PSO controller of the HAPF instantaneously detects the changes in the line currents and modifies the reference signals accordingly.

Fig. 7 (a) and (b) also show the waveforms of three-phase load and source currents under this case respectively. It is observed that the load currents take nearly 30ms to settle to new steady state value. The HAPF continuously track load currents and keep the source currents nearly sinusoidal. Experimentally it is observed that the source currents become instantaneously sinusoidal as soon as the HAPF is started as shown in Fig. 8, the starting of HAPF produces no transient currents. The maximum deviation in magnitude of fundamental source currents is within 100m.

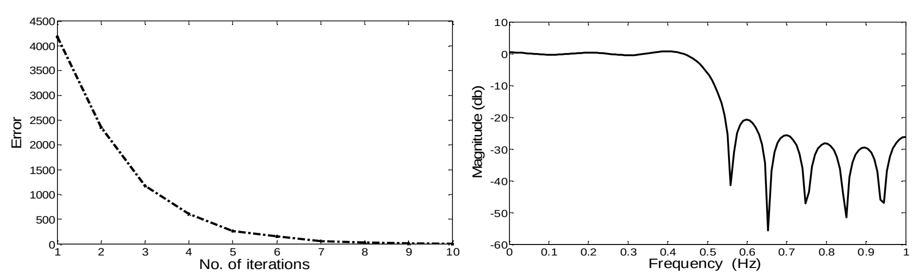

(a) (b)

Fig. 4. PSO filter responses (a) Error convergence plot, (b) Frequency response

Circuit parameter	Value
AC supply voltage (V$_s$)	240 V$_{rms}$
Frequency (f)	50 Hz
Source Resistance (R$_s$)	0.3 Ω
Source Inductance (L$_s$)	0.5 mH
Switching Frequency (f$_{sw}$)	12kHz
Gain (K)	30
DC link voltage (V$_{dc}$)	300 Volts
Switching filter (L$_f$, C$_f$)	12mH, 0.1uF
Coupling Transformer	Ratio 10:1

(a) (b)

Fig. 5(a) . Experimental setup; (b) Design specifications and circuit parameters

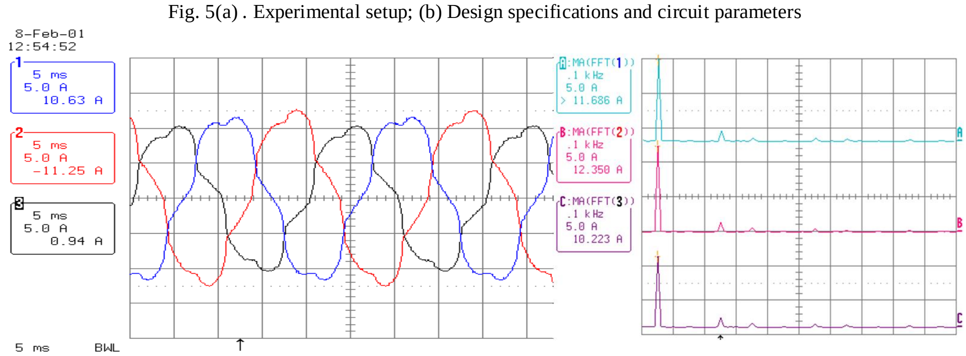

(a) (b)

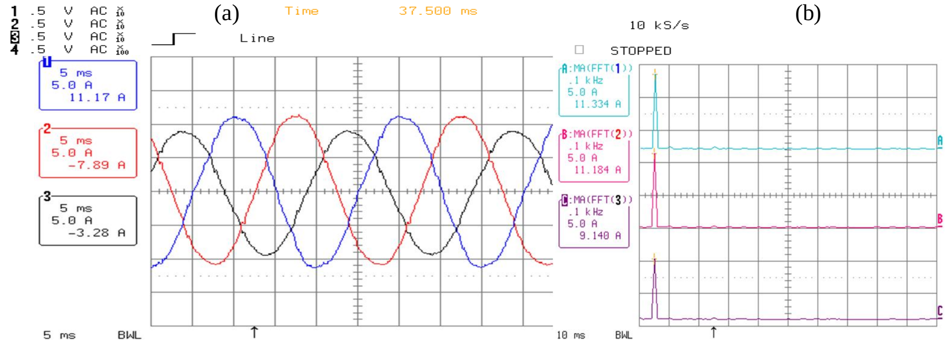

(c) (d)

Fig. 6 (a). 3-ph load currents (R +L+ Motor) load, (b). FFT of load currents (R +L+ Motor) load, (c). Source currents after harmonic compensation (R +L+ Motor) load, and (d). FFT of source current (R +L+ Motor) load

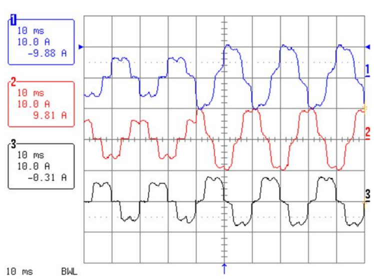

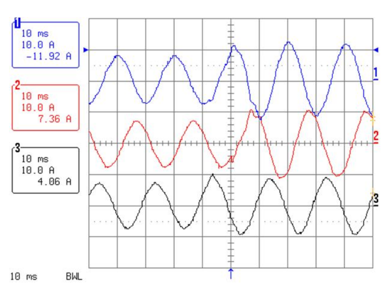

(a) (b)

Fig. 7 (a). Load currents with harmonic compensation on with (R+L) load, and (b). Source currents with harmonic compensation on with (R+L) load

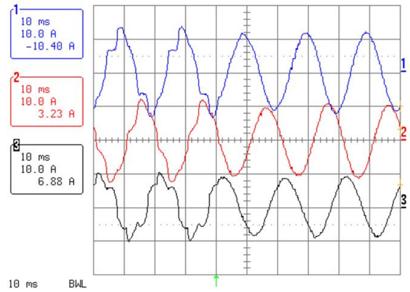

Fig. 8. Starting response with Rect+RL load and harmonic compensation

IV. Conclusions

In this paper a new control technique based on particle swarm optimization has been presented. The simulated results demonstrated its effectiveness under various operating conditions. Some of the advantages of the proposed controller are:

- It is independent of source voltage distortion and unbalance,
- Fast and accurate tracing of fundamental component under balanced and unbalanced nonlinear conditions,
- Simple architecture and easy for implementation, and
- The performance of the proposed system is being investigated under power system frequency variation and the results would be reported in near future.

Acknowledgment

This research work was supported by the AICTE under Research Promotion Scheme Grant Number 8023/RID/RPS-56 Pvt. The work has been carried out at Rungta College of Engineering and Technology, Bhilai, India during 2013-16.

References

[1] H. Akagi, "Trends in active power line conditioners," IEEE Trans. Power Electron., vol. 9, no. 3, pp. 263-268, May 1994.

[2] W. M. Grady, M. Samotyj and A. H. Noyola, "Survey of active power line conditioning methodologies," IEEE Trans. Power Del., vol. 5, no. 3, pp. 1536-1542, 1990.

[3] F. Peng, H. Akagi and A. Nabae, "A new approach to harmonic compensation in power systems-A combined system of shunt passive and series active filters," IEEE Trans. Ind. Appl., vol. 26, no. 6, pp. 983-990, Nov/Dec 1990.

[4] R. E. Shatshat, M. Kazerani and M. M. A. Salama, "Modular active power-line conditioner," IEEE Trans. Power Del., vol. 16, no. 4, pp. 700-709, Oct 2001.

[5] J. H. Marks and T. C. Green, "Predictive transient-following control of shunt and series active power filters," IEEE Trans. Power Electron, vol. 17, no. 4, pp. 574-584, Jul 2002.

[6] M. Rukonuzzaman and M. Nakaoka, "Magnitude and phase determination of harmonic currents by adaptive learning back-propagation neural network," in IEEE International Conference on Power Electronics and Drive Systems (PEDS '99), 1999.

[7] M. Jha and S. Dubey, "Neuro-Fuzzy Based Controller For A Shunt Active Power Filter," in International Conference on Power and Energy Systems (ICPS 2011), 22-24 Dec. 2011, 2011.

[8] N. Gupta, S. P. Dubey and S. Singh, "Neural network based shunt active filter for harmonic and reactive power compensation under non-ideal mains voltage," in 5th IEEE Conference on Industrial Electronics and Applications (ICIEA 2010), 5-17 June 2010, 2011.

[9] N. Gupta, S. P. Dubey and S. Singh, "Neural network-based shunt active filter with direct current control for power quality conditioning," IJPELEC, pp. 597-620, 2011.

[10] P. Singh, "Compensation of reactive and harmonic power in three-phase power system," Ph.D. thesis, IIT Delhi, Delhi, 2001.

[11] B. R. Lin, B. R. Yang and H. R. Tsai, "Analysis and operation of hybrid active filter for harmonic elimination," Elect. Power Syst. Res., vol. 62, no. 3, pp. 191-200, 2002.

[12] P. Singh, J. M. Pacas and a. R. Verma, "Control Scheme for Selective Compensation of Reactive Power under Distorted and Unbalanced Source," in European Conference on Power Quality (PCIM 2001), Germany, 2001.

[13] V. F. Corasaniti, M. Barbieri, P. Arnera and M. Valla, "Hybrid Active Filter for Reactive and Harmonics Compensation in a Distribution Network," IEEE Trans Ind Electron, vol. 56, no. 3, pp. 670-677, Mar 2009.
[14] R. L. d. A. Ribeiro, C. C. d. Azevedo and R. M. d. Sousa, "A robust adaptive control strategy of active power filters for power-factor correction; harmonic compensation; and balancing of nonlinear loads," IEEE Transactions on Power Electronics, vol. 27, no. 2, pp. 718-730, Feb 2012.
[15] Y. Tan and Y. Shi, "Special Issue on Advances in Swarm Intelligence: Theories; Algorithms and Applications: Guest Editorial Preface," International Journal of Swarm Intelligence Research, vol. 4, no. 1, pp. 1-132, 2013.
[16] J. J. Liang, A. K. Qin and P. Suganthan, "Comprehensive learning particle swarm optimizer for global optimization of multimodal functions," IEEE Trans. Evol. Comput., vol. 10, no. 3, pp. 281-295, Jun 2006.
[17] S. Mandal, P. Mallick, D. Mandal, R. Kar and S. P. Ghoshal, "Optimal FIR band pass filter design using novel particle swarm optimization algorithm," in IEEE Symposium on Humanities, Science and Engineering Research (SHUSER), 24-27 Jun. 2012, 2012.
[18] Z. Yu, "Symmetric PWM Outputs Generation with the TMS320C14 DSP," 1997. [Online]. [Accessed 6 Mar 2015].
[19] S. H. Kim and K. Ishiyama, "Hybrid Speed Control of a DC Motor for Magnetic Wireless Manipulation Based on Low Power Consumption: Application to a Magnetic Wireless Blood Pump," IEEE Transactions on Magnetics, vol. 50, no. 4, pp. 1-7, 2014.
[20] W. Li, Y. Niimi, Y. Orino, S. Hirata and M. K. Kurosawa, "A Frequency Synchronization Method for a Self-Oscillating PWM Signal Generator," IEEE Transactions on Circuits and Systems II: Express Briefs, vol. 61, no. 4, pp. 244-248, Apr 2014.
[21] S. E. Moya, J. Vilar, R. Korpys and J. Kolodziej, "Frequency and Total Harmonic Distortion Estimation Based on Adaptive Filters," IEEE (Revista IEEE America Latina): Latin America Transactions, vol. 11, no. 1, pp. 207-212, Feb 2013.